

Supporting Information Available

Charge Photo-Accumulation and Photocatalytic Hydrogen Evolution Under Visible Light at an Iridium(III)-Photosensitized Polyoxotungstate

Benjamin Matt, Jennifer Fize, Jamal Moussa, Hani Amouri, Alexandre Pereira, Vincent Artero, Guillaume Izzet, Anna Proust

Contents:

1. General methods

2. **Figure S1.** Experimental set up for the irradiation test of samples. reaction conditions: photocatalyst (0.2 mM), DMF (8.6 mL), triethylamine (1.4 mL, 1 M) and acetic acid (0.1 M, 500 equiv). Left: before irradiation, middle: one-electron reduced POM, right: two-electron reduced POM.

3. **Figure S2.** Spectroelectrochemical reduction of the POM reference **D_{Si}[I]**.

4. **Figure S3.** Evolution of the differential visible absorption spectrum of a solution of **D_{Si}[Ir]** (0.2 mM) in DMF containing TEA (1 M) and AcOH (0.1 M) during photoirradiation (dashed: theoretical absorption of the one-electron reduced species t = 65 sec, bold: t = 11 min). These spectra have been measured using the setup shown in Figure S1.

5. **Figure S4.** Left) Comparison of the ¹H NMR spectra of a 1 mM CD₃CN solution of **D_{Si}[Ir]**; before (black) and after addition of TEA (1M) / AcOH (0.1 M) (red). Right) Evolution of the ³¹P NMR spectrum of a 1 mM CD₃CN solution of **D_{Si}[Ir]** during the photolysis; a) before addition of TEA/AcOH; b) after addition of TEA (1M) / AcOH (0.1 M); c) after one hour of photolysis; d) after 20 hours of photolysis.

General methods.

Compounds **D_{Si}[Ir]**, **D_{Si}[I]** and **[Ir]** were prepared according to the previously reported synthetic route.¹

All electrochemical measurements were carried out under nitrogen at room temperature. Cyclic voltammetry was carried out using an Autolab PGSTAT 100 workstation and a standard three-electrode configuration consisting of glassy carbon or platinum disks (2 mm in diameter) as working electrode, an auxiliary platinum wire and a saturated calomel electrode. The supporting electrolyte was a 0.1 M solution of TBAPF₆ in DMF. Addition of acetic acid was made by syringe.

Bulk electrolysis experiments and coulometry were carried out on a BioLogic SP-300 instrument equipped with a 1A/48V booster. Rotating disk electrode experiments were controlled by a Radiometer analytical CTV101 control unit. A custom electrolysis cell was used, in which a Hellma 661.202-UV all-quartz immersion UV-visible probe (1 mm optical path length) and a Radiometer analytic EDI101 rotating platinum (2 mm in diameter) disk electrode can be simultaneously dipped into the electrolytic solution. A mercury pool (~5 cm²) was used as the working electrode and a Ag/AgCl/aqueous AgCl_{sat} + KCl 3 mol.L⁻¹ (denoted as Ag/AgCl throughout the text) closed by a Vycor frit and dipped directly into the solution was used as the reference electrode. The platinum-grid counter electrode was placed in a separate compartment connected by a glass-frit and filled with the supporting electrolyte. The supporting electrolyte was a 0.1 mol.L⁻¹ solution of TBAPF₆ in DMF.

UV-visible spectra were recorded with a Shimadzu UV-1800 spectrophotometer connected to a Hellma 661.202-UV all-quartz immersion UV-visible probe (1 mm optical path length) via a Hellma 662.000-UV/NIR Fibre-Optic Cable Interface and 2m long 041.102-UV quartz optic fibres. Photocatalytic experiments were carried out in a Schlenk tube made of pyrex. The samples were illuminated with a 300 W xenon lamp (Oriel, ozone free) operating at 280 W coupled with a water-filled Spectra-Physics 61NS liquid filter for elimination of IR radiations and a Spectra-Physics 59472 UV cut-off filter (lambda >400 nm). Irradiance was measured to 600 mW/cm² (~6 sun) thanks to a Coherent PowerMax-USB PM150-50C Power Sensor. In a typical experiment, the Schlenk tube (50 cm³) was filled with the photocatalyst (0.2 mM), DMF (8.6 mL), triethylamine (1.4 mL, 1 M) and acetic acid (0.1 M, 500 equiv.). The solution was thoroughly degassed by bubbling nitrogen and irradiated under stirring. Head-space gas samples (50 µL) were successively taken using a gas-tight syringe and analyzed using a Perkin-Elmer Clarus 500 gas chromatograph equipped with a porapak Q 80/100 column (6' 1/8") thermostated at 40 °C and a TCD detector thermostated at 100 °C. The mean area was used to determine the volume of hydrogen produced, knowing the total volume of the reactor, from a calibration curve.

¹ (a) B. Matt, X. Xiang, A. L. Kaledin, N. Han, J. Moussa, H. Amouri, S. Alves, C. L. Hill, T. Lian, D. G. Musaev, G. Izzet, A. Proust *Chem. Sci. accepted*,. (b) B. Matt, S. Renaudineau, L.-M. Chamoreau, C. Afonso, G. Izzet, A. Proust *J. Org. Chem.* **2011**, 76, 3107–3112. (c) B. Matt, J. Moussa, L. M. Chamoreau, C. Afonso, A. Proust, H. Amouri, G. Izzet *Organometallics* **2012**, 31, 35–38.

The ^1H (300.13 MHz), and $\{^1\text{H}\} \text{ } ^{31}\text{P}$ (121.5 MHz) NMR spectra were obtained at room temperature in 5 mm o.d. tubes on a Bruker Avance II 300 spectrometer equipped with a QNP probehead.

Quantum yields for the photoreduction were measured using an irradiation test bench shown in Figure S1. The main elements of the apparatus are a tightly closed quartz cell (sample volume 1 mL; path length = 1cm), a 1000W LSH502 xenon lamp and a Cornerstone 74000 1/8m monochromator. The image of the monochromator beam output is created on the front cell surface with a confocal optical system. For each wavelength, the average output power is measured using a Newport 1830c power-meter, and the focused beam area is estimated thanks to a CCD camera. The beam area is a spot of $\sim 5 \text{ mm} \times 1 \text{ mm}$. For a 400nm-wavelength, the average output power over the entire beam area is $\langle P \rangle = 195 \pm 5 \text{ } \mu\text{W}$. The same power measured after passing through the quartz cell filled with a DMF/TEOA (1M) solution is $153 \pm 5 \text{ } \mu\text{W}$. When a 0.2 mM sample of $\text{D}_{\text{Si}}[\text{Ir}]$ in a well-degassed DMF/TEAO (1M) solution is placed in the quartz cell, the output power measured after the cell is only $3.0 \pm 0.1 \text{ } \mu\text{W}$. We then took a value of $150 \text{ } \mu\text{W}$ for the light (400 nm) absorbed by the sample, yielding a flux of $5 \cdot 10^{10} \text{ photons}\cdot\text{s}^{-1}$. The amount of reduced $\text{D}_{\text{Si}}[\text{Ir}]$ is estimated from the measurement of the UV-visible spectra of the sample after various irradiation times under moderate stirring conditions. The quantum yield is determined by dividing the amount of reduced $\text{D}_{\text{Si}}[\text{Ir}]$ by the amount of 400 nm-photons absorbed by the sample.

The formation kinetics of the one-electron and two-electron reduced species have been evaluated by monitoring the visible absorption spectra of the photolyzed solution. We assume that the system is under thermodynamic control. As a consequence, the initial oxidized $\text{D}_{\text{Si}}[\text{Ir}]$ species can not coexist with the two-electron reduced species, $2\text{e}^- \text{-D}_{\text{Si}}[\text{Ir}]$ (they disproportionate into $1\text{e}^- \text{-D}_{\text{Si}}[\text{Ir}]$).

In the absence of acetic acid, for $t \leq 130 \text{ s}$, the absorption spectra have an identical profile with a growing absorbance and a maximum at 840 nm, attributed to the formation of $1\text{e}^- \text{-D}_{\text{Si}}[\text{Ir}]$. For $t > 130 \text{ s}$, an additional component appears at 720 nm, attributed to $2\text{e}^- \text{-D}_{\text{Si}}[\text{Ir}]$. These maximum absorption values are very close to those obtained from spectroelectrochemical measurements of the appropriate reference ($\lambda_{\text{max}, 1\text{e}^- \text{-D}_{\text{Si}}[\text{Ir}]} = 840 \text{ nm}$, $\lambda_{\text{max}, 2\text{e}^- \text{-D}_{\text{Si}}[\text{Ir}]} = 710 \text{ nm}$).

At $t = 130 \text{ s}$, only $1\text{e}^- \text{-D}_{\text{Si}}[\text{Ir}]$ is present. We can extract the extinction coefficient of this species ($\epsilon_{1\text{e}^- \text{-D}_{\text{Si}}[\text{Ir}]}(840) = 7600 \text{ M}^{-1}\cdot\text{cm}^{-1}$, $\epsilon_{1\text{e}^- \text{-D}_{\text{Si}}[\text{Ir}]}(720) = 5800 \text{ M}^{-1}\cdot\text{cm}^{-1}$). For $t > 1 \text{ hour}$, the absorption of the solution remains constant. We can therefore assume that at $t = 1 \text{ hour}$, only $2\text{e}^- \text{-D}_{\text{Si}}[\text{Ir}]$ is present and we can extract the extinction coefficient of this species: $\epsilon_{2\text{e}^- \text{-D}_{\text{Si}}[\text{Ir}]}(720) = 15400 \text{ M}^{-1}\cdot\text{cm}^{-1}$. The formation of $1\text{e}^- \text{-D}_{\text{Si}}[\text{Ir}]$ is followed at 840 nm for $t \leq 130 \text{ s}$, while the formation of $2\text{e}^- \text{-D}_{\text{Si}}[\text{Ir}]$ is followed at 720 nm for $t > 130 \text{ s}$.

The same procedure was performed to evaluate the photoreduction kinetics in the presence of acetic acid. The absorbance properties of the reduced species are slightly changed due to the protonation of the POM. The formation of $1\text{e}^- \text{-D}_{\text{Si}}[\text{Ir}]$ is followed at 845 nm for $t \leq 65 \text{ s}$, while the formation of $2\text{e}^- \text{-D}_{\text{Si}}[\text{Ir}]$ is followed at 695 nm for $t > 65 \text{ s}$. The calculated extinction coefficient of both reduced species are $\epsilon_{1\text{e}^- \text{-D}_{\text{Si}}[\text{Ir}]}(845) = 7100 \text{ M}^{-1}\cdot\text{cm}^{-1}$, $\epsilon_{1\text{e}^- \text{-D}_{\text{Si}}[\text{Ir}]}(695) = 4900 \text{ M}^{-1}\cdot\text{cm}^{-1}$, $\epsilon_{2\text{e}^- \text{-D}_{\text{Si}}[\text{Ir}]}(695) = 14400 \text{ M}^{-1}\cdot\text{cm}^{-1}$.

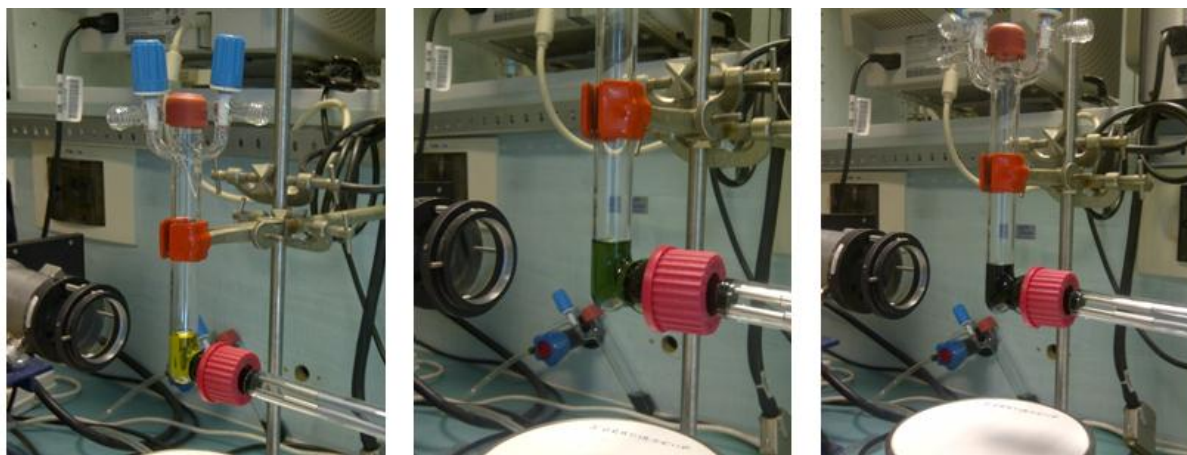
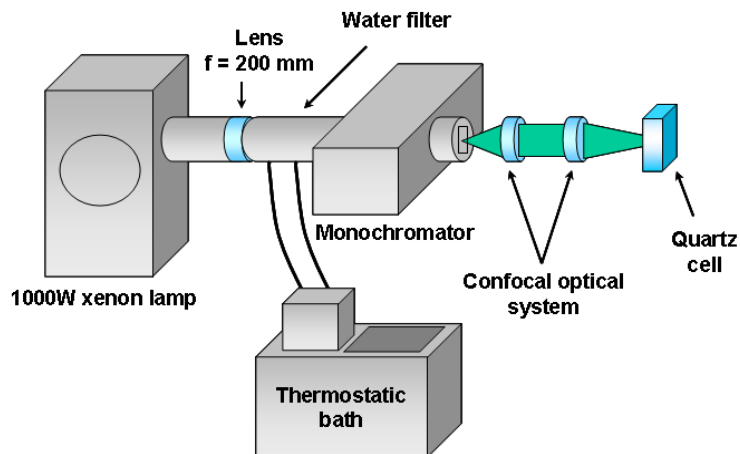


Figure S1. Top: Experimental set up for the irradiation test of samples, reaction conditions: photocatalyst (0.2 mM), DMF (8.6 mL), triethylamine (1.4 mL, 1 M) and acetic acid (0.1 M, 500 equiv). Down, left: before irradiation, down-middle: one-electron reduced POM, down-right: two-electron reduced POM.

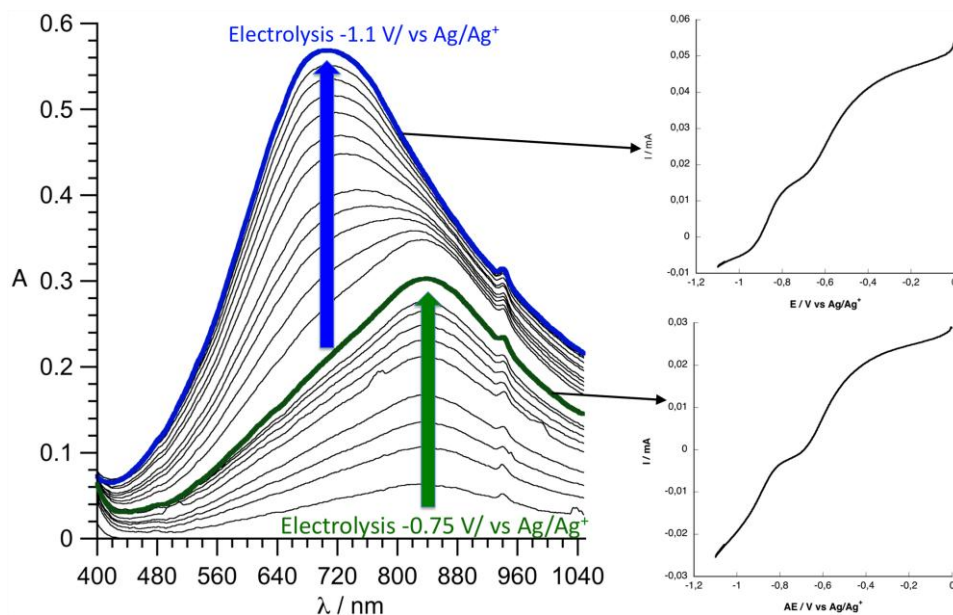


Figure S2. Left) spectroelectrochemical reduction (-0.75 V vs Ag/AgCl then -1.1 V vs Ag/AgCl) of the POM reference $\text{D}_{\text{Si}}[\text{I}]$ 0.5 mM in DMF containing 0.1 M $(\text{n-Bu}_4\text{N})\text{BF}_4$. Right) Rotating disk electrode voltammograms of the solution at different times. Down: after 1.8 C current exchange holding the potential at -0.75 V vs Ag/AgCl, formation of *ca.* 95% of the one-electron reduced POM (bold green curve, left). Top: after additional 1.8 C current exchange holding the potential at -1.1 V vs Ag/AgCl, formation of *ca.* 85% of the two-electron reduced POM (bold blue curve, left).

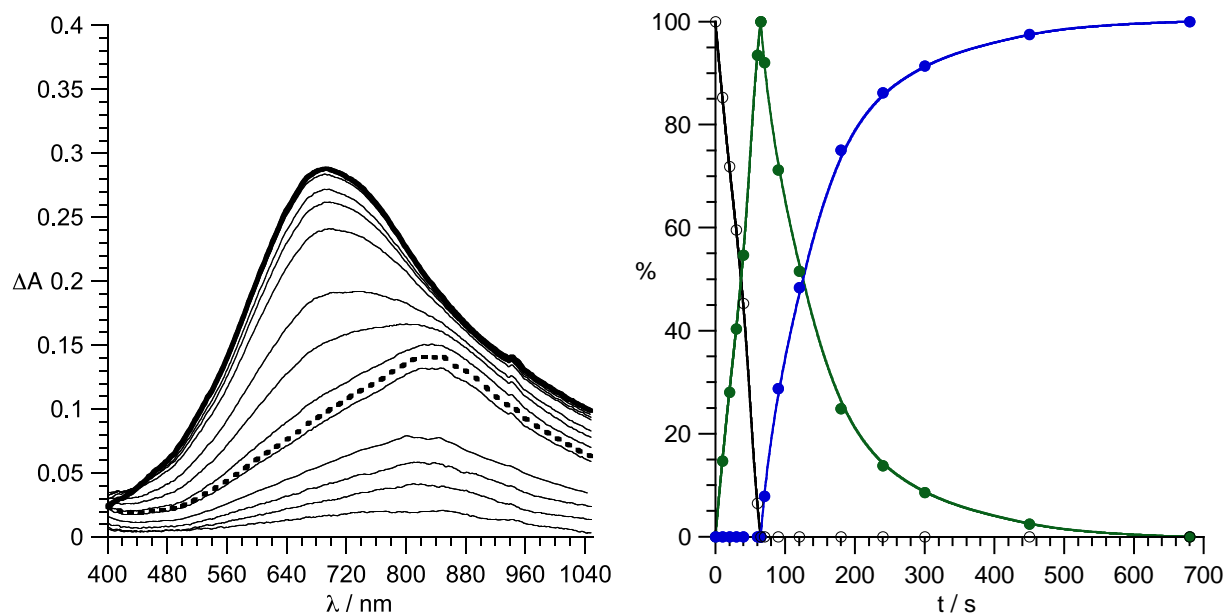


Figure S3. Left: evolution of the differential visible absorption spectrum of a solution of $\text{DSi}[\text{Ir}]$ (0.2 mM) in DMF containing TEA (1 M) and AcOH (0.1 M) during photoirradiation (dashed: theoretical absorption of the one-electron reduced species $t = 65$ sec, bold: $t = 11$ min). These spectra have been measured using the setup shown in Figure S1. Right: distribution of the different reduction states of $\text{DSi}[\text{Ir}]$ during the photolysis. Legend: non-reduced $\text{DSi}[\text{Ir}]$ (colorless circle), $1e^- \text{-DSi}[\text{Ir}]$ (green circle) and $2e^- \text{-DSi}[\text{Ir}]$ (blue circles).

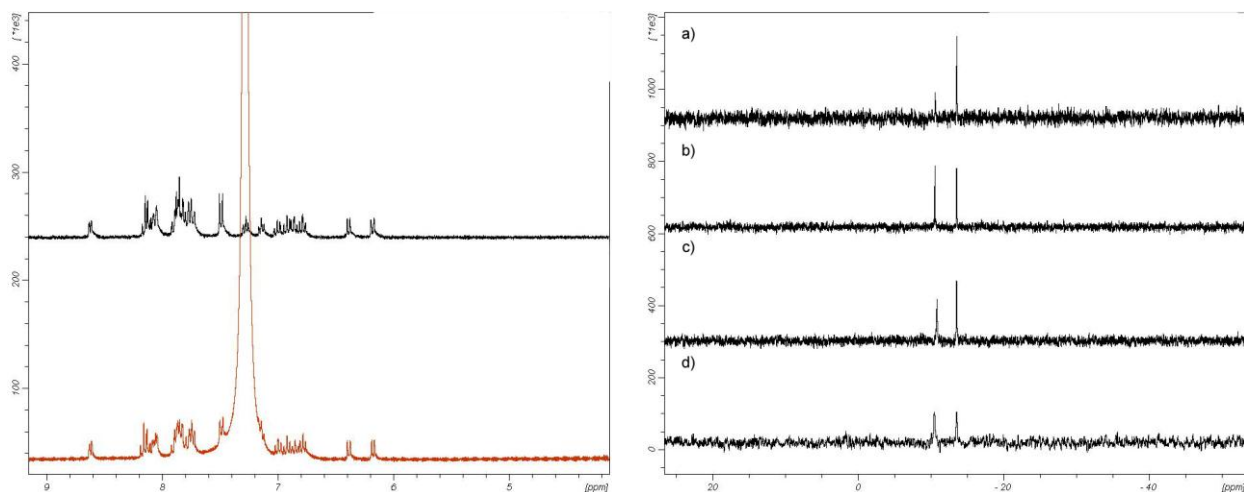


Figure S4. Left) Comparison of the ¹H NMR spectra of a 1 mM CD₃CN solution of **D_{Si}[Ir]**; before (black) and after addition of TEA (1M) / AcOH (0.1 M) (red). Right) Evolution of the ³¹P NMR spectrum of a 1 mM CD₃CN solution of **D_{Si}[Ir]** during the photolysis; a) before addition of TEA/AcOH; b) after addition of TEA (1M) / AcOH (0.1 M); c) after one hour of photolysis; d) after 20 hours of photolysis.